Respiratory Research

RESEARCH

Open Access

ETS2 aggravate allergic airway inflammation by regulating ANT2-mediated cytosolic mitochondrial DsRNA levels

Hui Jiang[1], Yaona Jiang[2], Ran Dong[3] and Chang-Yong Fu[4*]

Abstract

Background ETS2 has been identified as a pivotal regulator in the development of human inflammatory diseases. Nevertheless, the functional aspects of ETS2 in asthma remain inadequately characterized. The release of mitochondrial dsRNA is recognized as an initiator of innate immune responses and implicated in intensifying inflammation triggered by alternative immunogens. The interplay between these mechanisms remains poorly understood, and only a limited number of direct targets that underpin the pro-inflammatory role of ETS2 have been identified.

Methods The expression of ETS2 in epithelial cells under immune responses was analyzed, and its effects on asthma progression were examined through clinical specimens, human bronchial epithelial cells, and an allergic asthma mouse model. Additionally, the potential involvement of adenine nucleotide translocase-2 in mediating the immune responses regulated by ETS2 was explored.

Results Increased expression of ETS2 in lung epithelial cells was observed in both asthma patients and ovalbumin (OVA)-induced asthma mice. The deficiency of ETS2 resulted in a substantial decline in inflammatory cell infiltration and markedly diminished IL-6, IL-5, and IL-13 levels in epithelial cells. Mechanistically, ETS2 overexpression was associated with elevated cytosolic mitochondrial RNA levels, whereas knockdown resulted in their suppression. Furthermore, adenine nucleotide translocase-2 (ANT2) expression was robustly upregulated by ETS2 through direct promoter binding. The advantageous effects of ETS2 on asthma development were abrogated in ANT2-deficient mice.

Conclusions The findings collectively underscore the role of ETS2 as an exacerbating factor in allergic airway inflammation during asthma progression, primarily by inducing ANT2 expression. Therapeutic targeting of epithelial ETS2 could represent a novel approach to asthma management.

Clinical trial number Not applicable.

Keywords ANT2, Asthma, ETS2, Mitochondrial DsRNA, Mitochondrial function

*Correspondence:
Chang-Yong Fu
shouyi2011@163.com
[1]Department of Respiratory Medicine, Shanghai East hospital, Tongji university School of Medicine, Pudong, Shanghai, China
[2]Department of Pulmonary and Critical Care Medicine, People's Hospital of Tiantai Country, Taizhou, China
[3]Department of Respiratory, Tongji Hospital, School of Medicine, Tongji University, Shanghai, China
[4]Department of Neurology, Tongji Hospital, School of Medicine, Tongji University, Shanghai, China

Background

Asthma is a widely prevalent chronic respiratory disorder that is defined by airway inflammation, heightened bronchial responsiveness, and intermittent airflow obstruction [1]. It impacts millions globally and presents substantial burdens on public health infrastructure. The etiology of asthma is complex and multifactorial, encompassing genetic susceptibility, environmental exposures, and immune system dysregulation. Certain genes have attracted attention in the genetic domain for their potential roles in modulating asthma risk and influencing disease mechanisms [2]. E26 transformation-specific 2 (ETS2), belonging to the ETS family of transcription factors, is recognized for its involvement in various cellular mechanisms encompassing proliferation, apoptosis, and differentiation [3, 4]. Contemporary investigations have emphasized the importance of ETS2 in inflammatory diseases, with a particular focus on asthma [5]. Emerging evidence indicates that ETS2 participates in immune response regulation and may affect the expression of crucial cytokines and chemokines associated with airway inflammation. However, its precise function within the pulmonary system and its viability as a treatment target for respiratory conditions remain insufficiently understood.

While earlier genetic studies, such as Baron et al.[5], found no significant association between ETS2 variants and asthma risk, emerging evidence suggests that ETS2 may regulate immune responses through mechanisms not captured by traditional genetic association approaches. For example, ETS2's role in mitochondrial homeostasis and dsRNA sensing could influence inflammatory pathways relevant to asthma pathogenesis independently of strong genetic susceptibility signals. This study explores ETS2's functional impact on mitochondrial dsRNA-driven inflammation, providing a mechanistic basis for its potential role in asthma and other immune-mediated diseases beyond what genetic association studies alone could reveal.

In this study, it was demonstrated that epithelial ETS2 expression is elevated in both asthma patients and ovalbumin (OVA)-induced mice. The absence of ETS2 in epithelial cells markedly inhibits asthma progression. Conversely, the overexpression of epithelial ETS2 aggravated allergic airway inflammation in an adenine nucleotide translocase-2 (ANT2)-dependent manner. These findings suggest that epithelial ETS2 serves a critical function in asthma pathogenesis.

Materials and methods

Patients

Individuals between 30 and 40 years of age diagnosed with allergic asthma ($n = 8$), together with demographically comparable non-atopic healthy subjects ($n = 8$), were selected from Tongji Hospital, Shanghai. Lung tissue samples were collected via bronchoscopy using forceps to access the bronchial airways (Supplement Table 2). The experimental protocol for this investigation was sanctioned by the Clinical Research Ethics Committee of Tongji Hospital, following the principles established in the 1964 Helsinki Declaration and its later modifications. Each participant provided signed informed consent documentation.

Lung tissue sample preparation

In line with previous descriptions, single-cell suspensions of lung tissue were prepared by mechanically and enzymatically digesting the lung biopsies [6]. In brief, the GentleMACS Tumor Dissociation Kit, human (Miltenyi Biotech) was utilized to digest about 15 lung samples per patient in compliance with the directions that were provided by the manufacturer. After being isolated, the biopsies are promptly rinsed using RPMI (Merck). Then, they are transferred to a gentleMACS C Tube with 4.7 mL of RPMI augmented with 200 µl of enzyme H, 100 µl of enzyme R, and 25 µl of enzyme A. The tissue was then initially mechanically disrupted via program h_tumor_01 on a gentleMACS Dissociator. Enzymatic digestion of samples was carried out for one hour at 37℃ with constant rotation utilizing the MACSmix Tube Rotator. The gentleMACS Dissociator was applied twice during this incubation period, once halfway through and once at the end of the process. The next step was to strain the cell suspension using a 70µM cell strainer. The cells (1×10^6 per mL scRNAseq) were assessed for viability by trypan blue exclusion staining and then promptly cryopreserved in sterile filtrated 10% dimethyl sulfoxide (DMSO)/fetal bovine serum (FBS).

After being rapidly thawed in a 37℃ water bath, cell suspensions from frozen lung biopsy samples were transferred to sterile tubes containing warm RPMI medium (10%FBS). The viability was increased by utilizing a Dea cell removal kit (Miltenvi cat#130-090-101) after rinsing and counting. For every sample, complementary DNA (cDNA) libraries were generated following the instructions provided in the Chromium Next GEM Single Cell 3' Reagent Kits V 3.1 (10×) Genomics Chromium Next GEM Single cell 3' user handbook. The Agilent TapeStation was used for quantifying the cDNA and quality control. Libraries were pooled after normalization and quantification using Illumina/ROX low and Kappa Biosystems, with each sample containing 40k reads. Illumina NovaSeq was employed to sequence pooled libraries in a 100-cycle sequencing run via the S2 NovaSeq 6000 Reagents V.1 kit.

Pseudotime analysis

Cells were ordered into a branched pseudotime trajectory using Monocle 3 and the analysis was restricted to the highly variable genes identified by Seurat. Monocle was used to test for a significant correlation between gene expression and pseudotime in each trajectory [7]. A gene was defined as significantly associated with pseudotime if its estimated q value was < 0.01.

Mouse strains and a murine model of allergic asthma

ETS2$^{fl/fl}$ mice were generated through CRISPR/Cas9 technology, specifically targeting exons 3–5 of the murine ETS2 gene in a C57BL/6J genetic background. Subsequently, these *ETS2*$^{fl/fl}$ mice underwent breeding with Scgb1a1-Cre transgenic mice (The Jackson Laboratory) to establish a strain exhibiting myeloid-specific ETS2 deletion (*ETS2*$^{fl/fl;\ Scgb1a1-IRES-cre}$). Both male and female *ETS2*$^{fl/fl;\ Scgb1a1-IRES-cre}$ and their littermate control mice (*ETS2*$^{fl/fl}$) were utilized in this investigation.

ANT2$^{fl/fl}$ mice were established via CRISPR/Cas9, which targets exon 2–7 of the ANT2 gene of mice in a C57BL/6J background. *ANT2*$^{fl/fl}$ mice were subsequently bred with Scgb1a1-Cre transgenic mice (The Jackson Laboratory) to produce offspring featuring myeloid-specific *ANT2* deletion (*ANT2*$^{fl/fl;\ Scgb1a1-IRES-cre}$). Both male and female *ANT2*$^{fl/fl;\ Scgb1a1-IRES-cre}$ and their littermate control mice (*ANT2*$^{fl/fl}$) were utilized in experimental procedures. Wild-type C58BL/6J specimens were sourced from the Model Organisms Center (Shanghai, China). The induction of allergic airway inflammation was achieved through intratracheal administration (i.t.) of OVA, comprising initial sensitization with 20 μg OVA in 30 μl saline on days 0 and 7, followed by daily challenges using 10 μg OVA in 30 μl saline from days 10 through 28. Experimental cells were harvested from female mice aged 6–8 weeks. All specimens were housed and maintained in pathogen-free facilities with unrestricted access to sustenance. These protocols were sanctioned by the Tongji University Institutional Animal Use and Care Committee.

BAL and histopathological analysis

The lungs underwent triple lavage utilizing 0.5 mL of chilled PBS comprising 2% fetal bovine serum (FBS), and the obtained BALF underwent centrifugation at 1,500 rpm (4 °C, 5 min). BALF supernatants were preserved for analyzing cytokines and chemokines, whereas cellular precipitates were suspended again in 500 μL sterile PBS. Microscopic slides prepared from BALF cell precipitates enabled quantification of total cells and leukocyte populations. For pathological assessment, blood was cleared from pulmonary tissues using PBS before fixation in 10% formalin (24–48 h). The specimens underwent dehydration, xylene treatment, and paraffin embedding. Thin sections of lung tissue (5 μm) were prepared, underwent hematoxylin and eosin (H&E) or periodic acid-Schiff (PAS) staining, and were examined using a light microscope (Leica DM6000B, Leica Microsystems Inc., Buffalo Grove, IL, USA).

Cell culture, transfection of plasmids, and ShRNAs

Human bronchial epithelial cells (BEAS-2B, ATCC) were cultured in DMEM (Gibco, USA) supplemented with 10% FBS (Excell Bio, Shanghai, China) under conditions of 37 °C and 5% CO_2. Transient transfection of plasmids and shRNA was conducted utilizing Lipofectamine 3000 reagent (Thermo) per the supplier's protocol. For each well of a 6-well plate, 1 μg of in vitro-synthesized shRNA was employed. The cells underwent collection 30 h following transfection for further examination. Permanent cell lineages were generated by introducing BEAS-2B cells with VSVg, Hit60 packaging vectors, and the desired plasmid utilizing TurboFect (Thermo). The resulting retroviruses were gathered and applied to infect target cells, succeeded by selection using 5 μg/mL puromycin.

Airway epithelial cell isolation

To purify primary airway epithelial cells, the lungs underwent perfusion via the right ventricle using buffered saline before careful extraction. Dispase solution (BD Bioscience, 2 mL) was administered into the lungs, which was succeeded by a 1% low-melting agarose (Invitrogen) application. The lung specimens were maintained at 37 °C during a 1-hour incubation period. Following incubation, the lung material underwent mincing and mechanical separation through 100 μm and 70 μm nylon filters. The obtained cell suspensions were cleansed using PBS containing 1% FBS and 100 units of DNase I, followed by exposure to red blood cell lysis buffer (Sigma-Aldrich) for 5 min. After washing and centrifugation, CD45 + cells were eliminated from the mixture through anti-CD45 microbead treatment and filtration using a MACS® Cell Separation Column (Miltenyi Biotech).

Adeno-associated viruses (AAVs)

Human ETS2 coding sequences were inserted into an AAV vector regulated by a mouse albumin promoter to construct AAV9-ETS2. AAV9-NULL (control), AAV9-cre, and AAV9-ETS2 were generated and titrated by Vector BioLabs. Before i.t. OVA administration, mice underwent intratracheal delivery of 2×10^{11} genome copies of the AAVs.

Flow cytometric analysis of single lung cells

To acquire single-cell suspensions from pulmonary tissue, the lungs underwent PBS perfusion, were cut into tiny pieces, and underwent digestion in DMEM medium containing 5% FBS, 1 mg/mL collagenase D (Roche,

Mannheim, Germany), and 30 μg/mL DNase I (Roche) for 30 min at 37 °C. The processed lung suspensions were passed through a 70-μm cell strainer (Corning Inc., New York, USA) and then exposed to red blood cell lysis buffer. The cellular precipitates were labeled with monoclonal antibodies specific to CD45, CD4, CCR4, and CXCR3. DRAQ7 was utilized to eliminate dead cells when necessary. The cellular subsets were examined using a FACSVia flow cytometer (BD Biosciences, San Jose, CA, USA) or a Navios EX flow cytometer (Beckman Coulter, Inc., Miami, FL, USA).

Quantitative real-time RT-PCR

Total RNA was isolated from lung tissues and cells utilizing QIAzol reagent (Qiagen Inc., Valencia, CA, USA) and subsequently reverse transcribed into complementary DNA with the PrimeScript™ RT MasterMix (Takara Bio Inc., Shiga, Japan). Quantitative real-time PCR was performed using SYBR Premix Ex Taq™ (Takara Bio Inc.). GAPDH served as the internal control, and relative gene expression levels were determined by the ΔΔCt approach. The sequences of primers are provided in Supplementary Table 1.

Western blot (WB) assays

WB assays were conducted on primary airway epithelial cells or BEAS-2B cells, as previously described. Antibodies against ETS2 (cat# ab219948), H3 (cat# ab1797), PGC1-α (cat# ab191838), TFAM (cat# ab307302), MFN2 (cat# ab124773), MFN1 (cat# ab221661), and MDA5 (cat# ab314014) were obtained from Abcam. The antibody for α-Tubulin (cat# NB100-690) was procured from Novus.

Chromatin immunoprecipitation (ChIP) assay

Lungs from mice administered with either AAV9-NULL or AAV9-ETS2 underwent homogenization in chilled 1× PBS containing protease inhibitor mixture (Roche, NJ), 2 μg/mL PMSF, 1 mM EDTA, and 1 mM EGTA. Chromatin immunoprecipitation was conducted utilizing a ChIP analysis kit (Cat# 17–295; Millipore, MA) with minor adjustments to the manufacturer's guidelines. Specifically, the pulmonary homogenate underwent filtration to eliminate debris and cross-linking with 1% formaldehyde. Following sonication and preliminary clearing with Protein A Agarose/Salmon Sperm DNA, the fragmented chromatin underwent immunoprecipitation using either an IgG or an anti-ETS2 antibody. Post-elution, the recovered DNA-antibody complex was processed with proteinase K. The isolated DNA underwent qPCR examination using primers encompassing the ETS2 binding region within the ANT2 promoter. The supernatant obtained before immunoprecipitation from each specimen served as its input reference.

Statistics

Every experimental procedure was replicated independently two to three times as biological duplicates. When not explicitly stated otherwise, all measurements are expressed as the mean ± SD. For comparisons between pairs of groups, statistical analysis utilized either a two-tailed Student's t-test or Mann-Whitney U test (non-parametric). To assess variations among multiple groups, one-way ANOVA was implemented, followed by Tukey's post hoc analysis. All statistical computations were executed using GraphPad Prism version 8.00 (GraphPad Software, San Diego, USA).

Results

Single-cell transcriptome profiling of airway mucosal cellular in human

Droplet-based scRNA-seq analysis (10× Genomics) was conducted on eight bronchus samples from asthma patients and eight bronchus samples from healthy donors. Following the application of an analysis pipeline to exclude low-quality cells, approximately 0.32 billion unique transcripts were procured from a total of 52,152 cells. Among these, 25,397 cells (48.7%) were derived from asthma patients, while 26,755 cells (51.3%) originated from healthy bronchus tissues of the control group. To provide an overview, seven major cell lineages were identified utilizing well-established markers, encompassing T cells, natural killer (NK) cells, B cells, epithelial cells, monocytes, dendritic cells (DCs), and macrophages (Fig. 1A and 1). Additionally, the relative proportions of B cells, DCs, and monocytes were elevated in asthma lung tissues, whereas the relative proportions of T cells and epithelial cells were reduced in comparison to healthy lung tissues (Fig. 1C-1).

Pseudotime analysis reveals the dynamic changes in cell subpopulations

To investigate potential developmental links within the epithelial clusters, trajectory analysis was conducted on clusters 1, 3, 5, 9, 12, and 15 utilizing the Monocle algorithm. Two branch points were identified utilizing variations in epithelial gene expression, which were visualized along pseudotime. The clusters were mapped onto the Monocle pseudotime plot, revealing that clusters 5 and 12 were situated at the initial stages of pseudotime (Fig. 2A-2). Notably, cluster 15 was distributed throughout the pseudotime trajectory, suggesting its possible involvement in epithelial cell differentiation pathways (Fig. 2C).

To further explore this, characteristic gene levels encompassing DYNLL1, ETS2, and TUBB4B were examined in cluster 15 along the pseudotime trajectory. These genes were found to exhibit markedly elevated expression levels (Fig. 2D), indicating their possible involvement

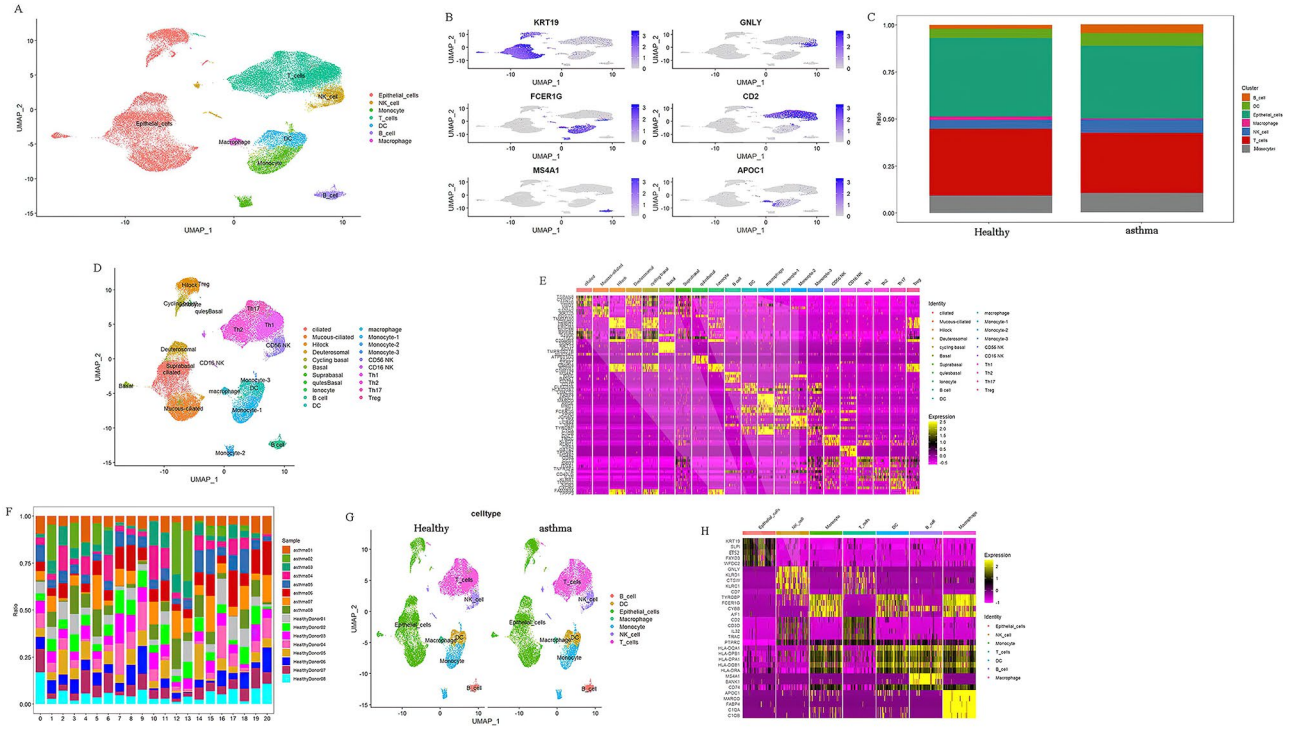

Fig. 1 Single-cell transcriptom proliling of airway mucosal cellular in human. (**A**) Cell populations identified by scRNA-seq in human lung tissues. The uniform manifold approximation and projection (UMAP) of 52,152 single cells from healthy lung ($n=8$) and asthma lung tissue ($n=8$) samples, and seven major cell clusters identified are labeled. Each dot corresponds to a single cell and is colored according to its cell type. (**B**) Canonical markers of different cell types were used to identify cell clusters as represented in the UMAP plot (**A**). (**C**)Average proportion of the different cell types in healthy lung samples ($n=8$) and asthma lung samples ($n=8$). (**D**) Clustering of 52,152 cells from early-stage asthma airway tissues ($n=8$) and healthy airway tissues ($n=8$). Each dot corresponds to a single cell and is colored according to the type of cell. Of the cells analyzed, 25,397 cells (48.7%) originated from lung cancer tissues, and 26,755 cells (51.3%) originated from healthy lung tissues. (**E**) Heatmap of cluster marker genes related to (A), with cell lineage of exemplar genes labelled (right). Columns denote cell subtypes and rows denote genes. (**F**) Sample distribution in each cell subtype. Each bar corresponds to one cell subtype, colored according to samples. (**G**) Annotation in UMAP plots in healthy airway tissues versus asthma airway tissues. (**H**) Shown is the heatmap of cluster marker genes of the 7 major cell lineages, with cell lineage of exemplar genes labeled

in the post-asthmatic differentiation of epithelial cells. Conversely, characteristic gene levels in cluster 3 decreased progressively with the pseudotime trajectory (Fig. 2D), implying a limited role in promoting airway inflammation.

Differentially expressed genes (DEGs) and enrichment analysis

Drawing from earlier findings (Fig. 2), it was identified that cluster 15 may serve a pivotal function in promoting airway inflammation. Consequently, whole-genome transcriptome analysis was conducted on cluster 15 from lung samples of asthma patients and controls. This analysis revealed 304 DEGs, encompassing 93 upregulated and 211 downregulated genes (Fig. 3A, $P<0.05$). Among these, ETS2 expression was found to be upregulated. Several of the top DEGs are known to participate in redox reactions (e.g., *TXN* and *ATP5F1E*), mitochondrial function regulation (e.g., *NDUFA1*, *ATP5MG*, and *ATP5MJ*), and immune regulation (e.g., *MCEMP1*, *IRAK3*, *FCER1G*, *LILRA5*, and *IL1R2*). To elucidate key biological processes and cellular pathways modified in asthmatic conditions, analyses utilizing gene ontology (GO) and the Kyoto Encyclopedia of Genes and Genomes (KEGG) were implemented. KEGG pathway assessment of upregulated transcripts (Fig. 2B) indicated oxidative phosphorylation as a crucial component in asthma development. Similarly, GO molecular function evaluation of elevated genes in asthmatic samples showed enrichment in OXPHOS-associated activities, encompassing electron transport functions, cytochrome-c oxidase processes, and NAD + nucleosidase operations (Fig. 2C). These observations suggest that impaired OXPHOS and mitochondrial activities significantly influence asthma progression. The transcriptional investigation revealed 304 differentially expressed genes in asthmatic subjects, potentially connected to redox processes, mitochondrial activities, and immune responses (Supplement 1). Enrichment evaluations further emphasized notable changes in the OXPHOS pathway (Figs. 2B and 2), emphasizing the significance of mitochondrial impairment in asthma manifestation.

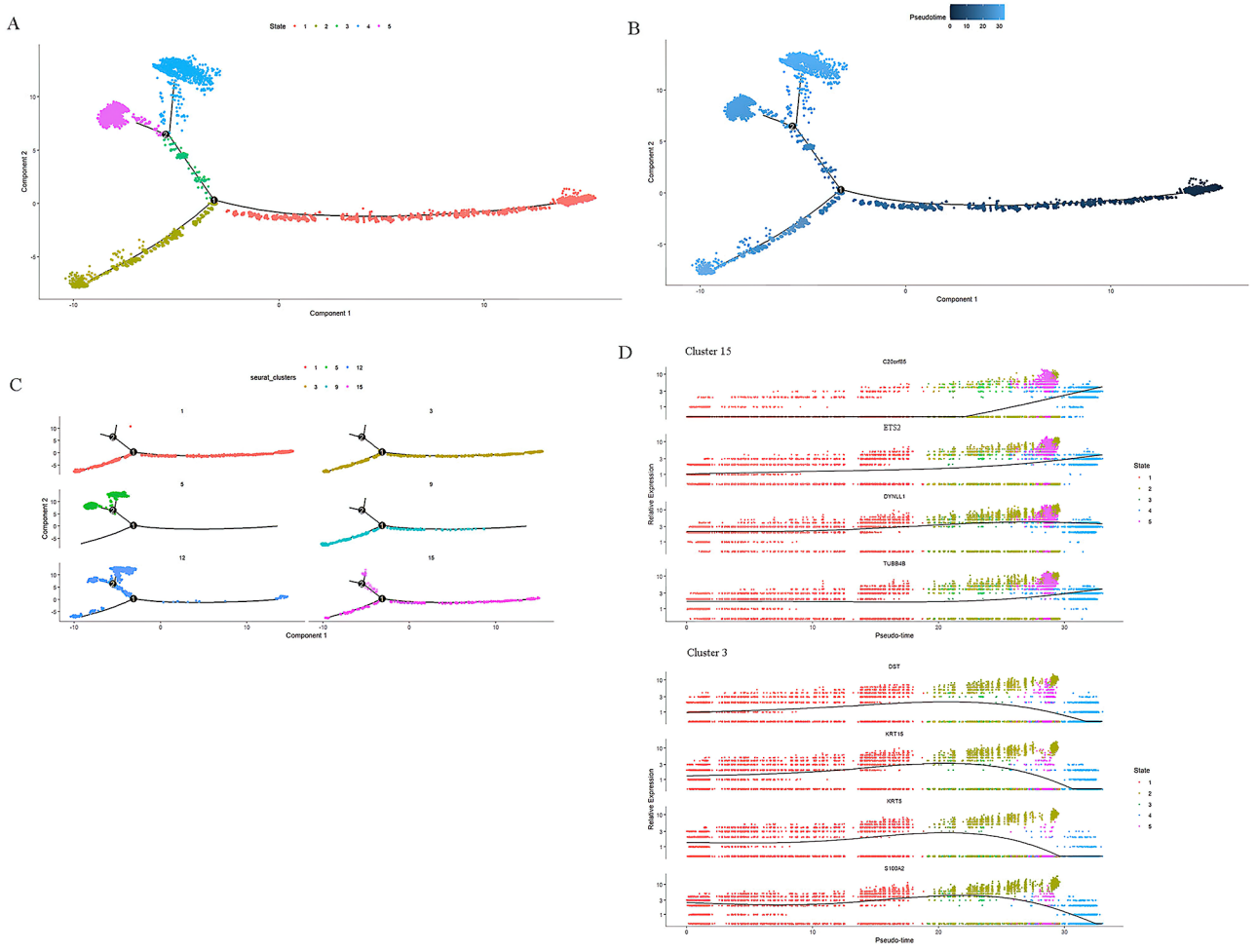

Fig. 2 Pseudotime analysis revealed the dynamic changes in cell subpopulation of Epithelial cells. (**A**) The Epithelial cell subgroups were selected for trajectory reconstruction. Pseudotime reconstruction revealed a bifurcation trajectory of epithelial cells development. The color of individual cells along the optimized embedding path represents the different states of epithelial cells differentiation. (**B**) The direction indicated by the arrow represents the trajectory of epithelial differentiation. (**C**) Distribution of different clusters of epithelial cells on the differentiation trajectory. (**D**) Dynamic changes in the expression of core genes involved in regulating the differentiation of different clusters

Bronchial epithelial cells ETS2 deficiency attenuates OVA-induced oxidative stress injury and mitochondrial dysfunction

To further investigate the role of ETS2 in asthma, a murine asthma model was developed utilizing WT C57BL/6 mice (Fig. 4A). Reverse transcription quantitative polymerase chain reaction validated the transcriptomic findings, demonstrating increased ETS2 mRNA expression in the epithelial cells of OVA-induced asthma mice (Fig. 4B). Elevated epithelial cells ETS2 protein levels (Fig. 4C), as well as increased nuclear ETS2 and phosphorylated ETS2 levels (Fig. 4D), were consistent with ETS2 activation. In agreement with observations from clinical samples, ETS2 mRNA expression was markedly higher in the asthmatic group ($P<0.001$; Fig. 4E). To assess the functional significance of ETS2 in lung disease, mice with lung epithelial cell-specific ETS2 deletion were generated, where ETS2 mRNA could not be amplified in healthy lung epithelial cells. H&E staining of lung tissues suggested that, at 30 days post-OVA induction, mice lacking ETS2 in epithelial cells exhibited markedly reduced infiltration of inflammatory cells (Fig. 4F). Bronchoalveolar lavage fluid (BALF) cell counts revealed that ETS2 deficiency markedly decreased the number of inflammatory cells ($P<0.05$; Fig. 4G). To explore the molecular mechanisms through which ETS2 deficiency alleviates bronchial epithelial cell injury, primary airway epithelial cells from $ETS2^{fl/fl}$ and $ETS2^{fl/fl;\ Scgb1a1\text{-}IRES\text{-}cre}$ mice were studied. ETS2 deficiency not only markedly reduced inflammatory cell infiltration but also suppressed the elevation of IL-33, IL-25, and TLSP levels in epithelial cells (Fig. 4H). Mitochondrial function has been implicated as serving a pivotal function in the development of airway allergic inflammation in asthma [8]. This investigation explored how ETS2 influences mitochondrial functionality in bronchial epithelial cells. According to Figs. 4I

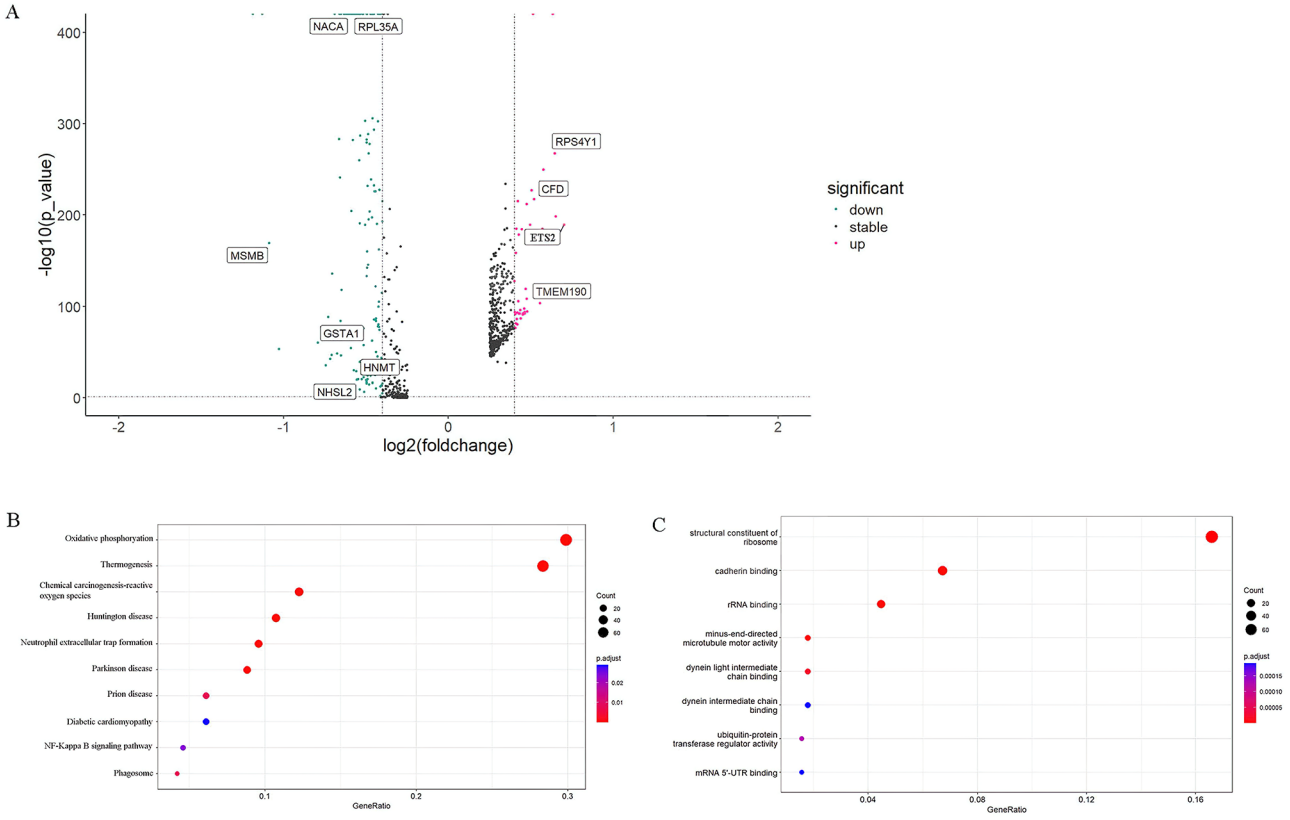

Fig. 3 Differentially expressed genes and enrichment analysis. (**A**) The volcano plots of DEGs in cluster 15 with asthma compare to control patients. (**B**) The top 10 KEGG pathways enrichment analysis of up regulate genes, (**C**) Top 8 enrichment terms in the molecular function (MF) in control and asthma patients

and 4, ETS2 absence significantly counteracted the OVA-induced decrease in both ATP levels and mtDNA replication numbers. Exposure to OVA considerably disrupted the mitochondrial biogenesis regulator PGC-1α along with its target proteins, specifically TFAM, MFN1, and MFN2, plus the fusion mediator OPA1. ETS2 deficiency was found to restore PGC-1α protein levels and rescue the reduction in TFAM and MFN1 levels (Figs. 4K and 4).

ETS2 derives mitochondrial DsRNA into the cytosol

Abnormal mtDNA discharge has been linked to inherited leiomyomatosis and kidney cell cancer, while elevated expression of mitochondrial antiviral signaling (MAVS) in the RNA-detecting immune signaling cascade augments the responsiveness of immune-resistant colorectal tumors to checkpoint inhibition therapy [9, 10]. Notably, fluctuations in ETS2 quantities affected the levels of mitochondrial RNAs present in the cytoplasm. Enhanced ETS2 expression in BEAS-2B cells triggered an elevation in cytoplasmic mitochondrial RNA content, while its suppression caused a reduction (Fig. 5A). It merits emphasis that cytoplasmic mitochondrial RNA and total mitochondrial dsRNA constitute just a minor fraction of the complete mitochondrial RNA pool [11]. Given that total mitochondrial RNA quantities stayed constant during ETS2 manipulation, shifts in cytoplasmic mitochondrial RNA suggest modified transport efficiency. Immunofluorescence utilizing a dsRNA-specific monoclonal antibody (J2) demonstrated parallel increases or decreases in dsRNA quantities following ETS2 enhancement or reduction, respectively (Fig. 5B, 5). Alterations in cytoplasmic mitochondrial dsRNA were mirrored in subsequent immune reactions, with MDA5, retinoic acid-inducible gene 1 (RIG-I), and interferon-stimulated gene 15 (ISG15) transcript levels showing elevation in cells with increased ETS2 and reduction in cells with decreased ETS2 (Fig. 5D). Comparable patterns emerged in the protein quantities of MDA5, RIG-I, and ISG15 (Fig. 5E).

ETS2 deficiency results in suppressed ANT2 expression

To examine ETS2's function in the inflammatory response of lung epithelial cells via mitochondrial dsRNA release, lung transcriptomic profiles were generated for $ETS2^{fl/fl}$ and $ETS2^{fl/fl;\ Scgb1a1-IRES-cre}$ mice with OVA-induced asthma. RNA sequencing identified 108 DEGs ($P < 0.05$), comprising 63 downregulated and 45

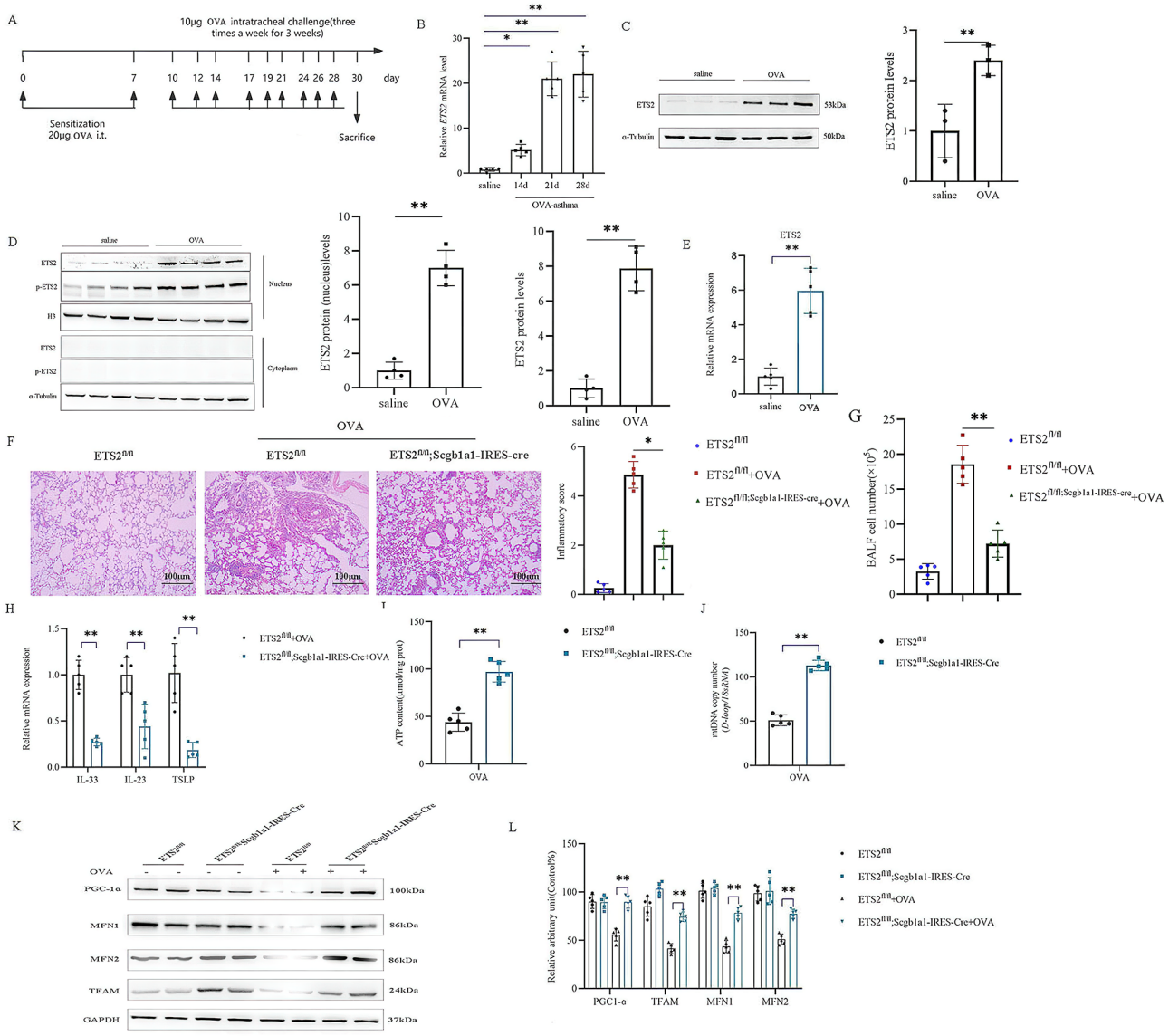

Fig. 4 Bronchial epithelial cells ETS2 deficiency attenuates OVA-induced oxidative stress injury and mitochondrial dysfunction. (**A**) Protocol for OVA-sensitised and OVA-challenged chronic mouse model. (**B**) In OVA-induced asthma, ETS2 mRNA (quantitative reverse transcription polymerase chain reaction) was already upregulated at 14days and peaked at 21 to 28 days. (**C**) Epithelial cell protein assessed by Western blot at 30 day following OVA-treatment. *$P < 0.05$ versus saline. (**D**) Western blot analysis of epithelial neulear and cytoplasmic ETS2 and phosphorylated (p-) ETS2 protein at 30 days following OVA-treatment or saline.*$P < 0.05$,**$P < 0.01$ versus saline. Mean ± SD of 3 to 6 animal per group. (**F**) Representative H&E images for the lung section of the *ETS2*$^{fl/fl}$ and *ETS2*$^{fl/fl;\ Scgb1a1-IRES-cre}$(scale bar = 50 μm). (**G**) Cell counts in BALF from mice. (**H**) Analyses of the transcription levels for IL-33, IL-25, and TLSP genes in each group through RT-qPCR. mRNA levels were normalised to the housekeeping gene,18s rRNA. (**I**) ATP content, (**J**) Relative mtDNA copy number, (**K**) Western blot image and (**L**) statistical analysis on relative protein content of PGC-1α,TFAM, MFN2,MFN1 in epithelial cells

upregulated genes in *ETS2*$^{fl/fl;\ Scgb1a1-IRES-cre}$ mice relative to *ETS2*$^{fl/fl}$ mice with asthma (Fig. 6A). Among the top 10 downregulated genes, all with a fold-change of < 0.50, were ANT2 (fold-change 0.48), MDA5, and retinoic acid-inducible gene 1 (RIG-I), which are downstream immune response genes in lung epithelial cells that exhibit reduced expression under conditions of ANT2 deficiency (Fig. 6B). ANT2, known to function as an RNA translocon, modulates immune responses by modulating cytosolic mitochondrial dsRNA levels. It has been demonstrated that decreasing ANT2 protein levels effectively reduces cytosolic mitochondrial dsRNA levels, alleviating inflammation in affected tissues. To further elucidate the interaction between ETS2 and ANT2, a more pronounced downregulation of ANT2 mRNA (Fig. 6C) and protein levels (Fig. 6D and 6) was observed in lung epithelial cells of *ETS2*$^{fl/fl;\ Scgb1a1-IRES-cre}$ mice with asthma compared to WT mice with asthma. These findings, confirmed by reverse transcription polymerase chain reaction, WB, and immunohistochemistry, suggest

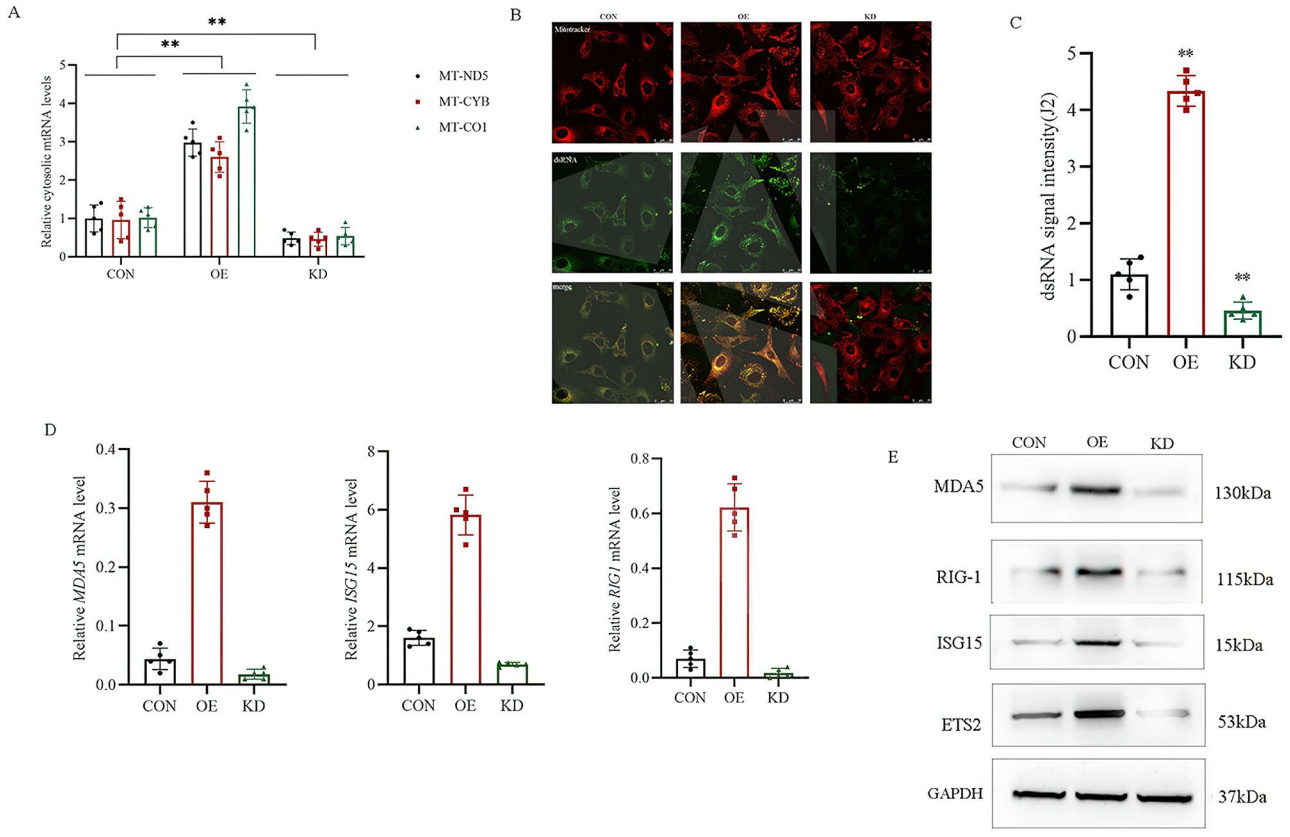

Fig. 5 ETS2 derives mitochondrial dsRNA into the cytosol. (**A**) Relative mitochondrial RNA levels in the cytosol of ETS2-overexpressing (OE),-knockdown (KD) or the vector-control (CON) cells. (**B**) Confocal examination of dsRNA levels in ETS2-overexpressing (OE),-knockdown (KD) or the vector-control (CON) cells with J2 antibody. (**C**) Quantification of the relative dsRNA fluorescent signals in B. (**D**) Relative ISG15,MDA5,RIG-1 mRNA levels in ETS-overexpressing (OE),-knockdown (KD) or the vector-control (CON) cells. (**E**). ISG15,MDA5,RIG-1and ETS2 protein levels in ETS-overexpressing (OE), -knockdown (KD) or the vector-control (CON) cells. GAPGH was used as a loading control

a potential role for endogenous ETS2 in maintaining ANT2 expression. Consequently, the possibility that ETS2 exacerbates asthma through the induction of ANT2 was further examined. We observed that the protein levels MDA5,RIG-1,ISG15 were significanliy decreased in $ETS2^{fl/fl;\ Scgb1a1-IRES-cre}$ mice with asthma (Supplementary Fig. 1A), the results showes that in vivo the expression trend of the MDA5,RIG-1 and ISG15 was consistent with the in vitro, with MDA5,RIG-1,ISG15 expression showing an positive relationship with ETS2 expression. Thus, the data suggest that ETS2 regulates immune responses (IL-33,IL-23 and TSLP) through mediating MDA5,RIG-1 and ISG15 levels in the cytosol. We performed rescure assay to identify the role of MDA5, RIG-1,ISG15 and ETS2 in the immune response of epithelial. siRNA was used to inhibit the expression of ETS2. Consistent with the previous results, we first observed that the mRNA expression of IL-33,IL-23 and TSLP decreased after the downregulation of ETS2 with OVA stimulation in BEAS-2B cells. Subsequently, we found that after transfection of the MDA5,RIG-1 and ISG15 overexpression plasmid, the decrease in the mRNA expression of IL-33,IL-23 and TSLP inhibited by siETS2 was reversed (Supplementary Fig. 1B). Airway epithelial cells release alarm hormones (IL-33, TSLP, and IL-25) that activate ILC2s and Th2 cells, creating a positive feedback loop.

ETS2 exacerbates asthma development via ANT2

Lung epithelial-specific $ANT2^{-/-}$($ANT2^{fl/fl;\ Scgb1a1-IRES-cre}$) mice and $ANT2^{fl/fl}$ mice were intratracheally injected with AAV9-Null or AAV9-hETS2, followed by OVA treatment for 30 days. As anticipated, overexpression of epithelial ETS2 in $ANT2^{fl/fl}$ mice markedly increased pro-inflammatory cytokines and chemokines, encompassing IL-6 and CXCL1, which were abolished in $ANT2^{fl/fl;\ Scgb1a1-IRES-cre}$ mice (Fig. 7A-7), indicating that ETS2's inflammatory activity requires ANT2. Notably, IL-5 and IL-13, two typical asthma-associated Th2 cytokines known to regulate airway obstruction, hyperreactivity, and remodeling [12], exhibited considerable elevates in the lungs following AAV9-ETS2 injection but were suppressed in $ANT2^{fl/fl;\ Scgb1a1-IRES-cre}$ mice. Consistent with the reduction in Th2 responses observed in $ANT2^{fl/fl;\ Scgb1a1-IRES-cre}$ mice, flow cytometric analysis

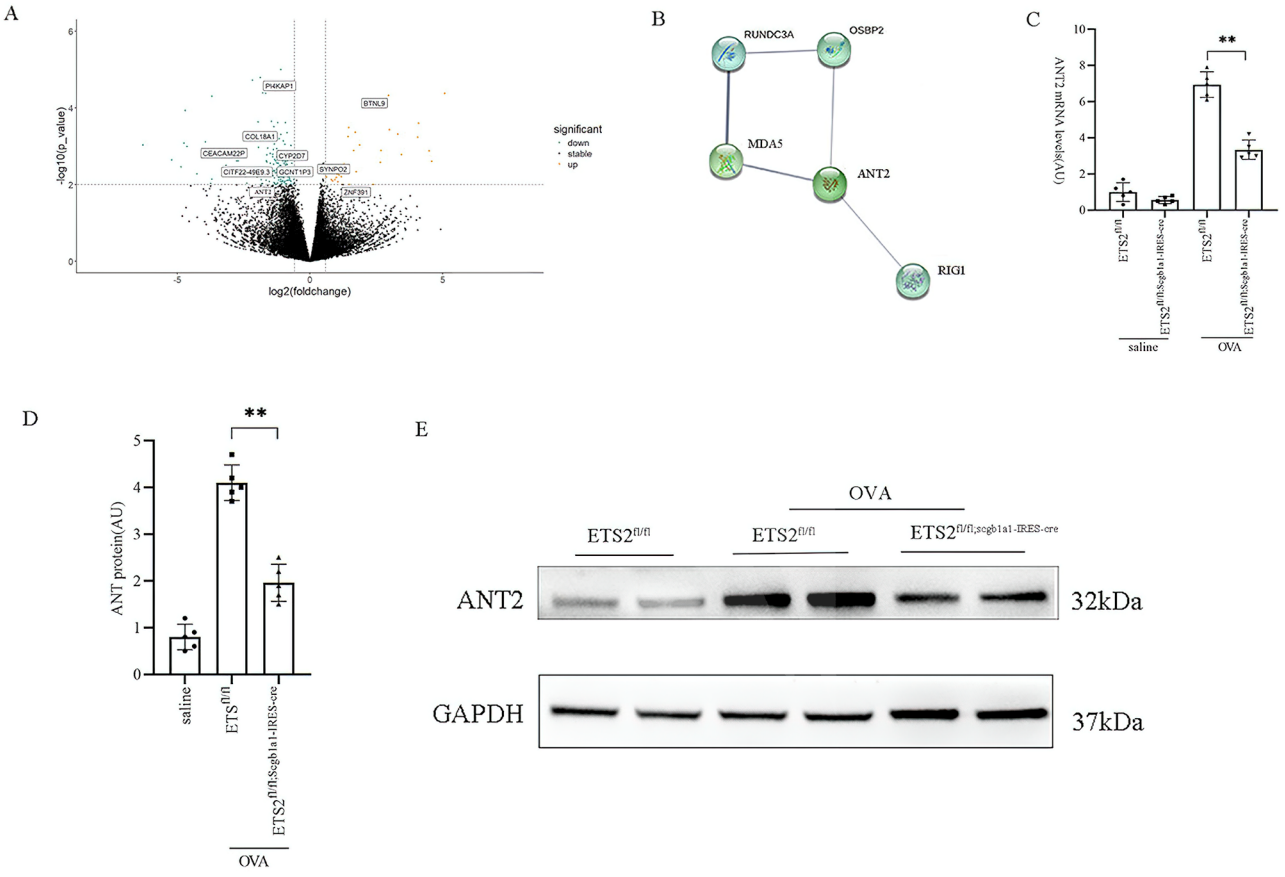

Fig. 6 ETS2 deficiency results in suppressed ANT2 expression. (**A**) The volcano plots of DEGs in *ETS2*$^{fl/fl}$ compared to *ETS2*$^{fl/fl}$;*Scgb1a1-IRES-cre* mice with OVA-induced asthma. (**B**) Input DEGs into ChEA3 (https://maayanlab.cloud/chea3) to obtain the downstream of ETS2. (**c**, **d**) Decrease epithelial ANT2 mRNA (**C**) and protein (**D**, **E**) expression in mice with genetically modified epithelial cells (*ETS2*$^{fl/fl}$;*Scgb1a1-IRES-cre* mice) with asthma compared to *ETS2*$^{fl/fl}$. $^{**}P < 0.01$ versus *ETS2*$^{fl/fl}$

showed a significant decrease in CCR4 + CXCR3- Th2 cells in the lungs of ANT2$^{fl/fl;\ Scgb1a1-IRES-cre}$ mice compared to ANT2$^{fl/fl}$ mice (Fig. 7E). We supplemented the study of eosinophilic infiltration in lung in ANT2 knockout model, to investigate how ETS2-dependent mitochondrial dsRNA in airway epithelia shapes the immune microenvironment, potentially through paracrine signaling to innate and adaptive immune cells (Fig. 7E). At the gene expression level, overexpression of epithelial ETS2 markedly increased the expression of cytosolic mitochondrial dsRNA-related genes (ND5, CYD, CO1) in ANT2$^{fl/fl}$ mice but not in ANT2$^{fl/fl;\ Scgb1a1-IRES-cre}$ mice (Fig. 7F). These gene expression changes align with the observed phenotypic alterations. Collectively, the data presented in Fig. 7 demonstrate that overexpression of epithelial ETS2 promotes asthma development through the induction of ANT2.

ANT2 is a direct target of ETS2

The data depicted in Fig. 7 indicate that epithelial ANT2 mediates the exacerbating effect of ETS2 on asthma. To further explore how ETS2 regulates ANT2 expression, BEAS-2B cells were transfected with an expression plasmid encoding ETS2, which markedly increased ANT2 promoter activities by over 3.7-fold at both the − 1.0 kb and − 0.3 kb regions (Fig. 8A-8). The transcriptional activation was entirely eliminated following mutation of the ETS2 recognition sequence positioned at -184 bp to -177 bp (Fig. 8C). Analysis of lung tissue utilizing ChIP methodology revealed direct ETS2 protein interaction with the corresponding ANT2 promoter segment (Fig. 8D; $P < 0.01$). Collectively, the data from Fig. 8 suggest that ANT2 is a direct transcriptional target of ETS2.

Discussion

This study explored the role of ETS2 in asthma. The primary findings can be summarized as follows: (1) ETS2 expression was elevated in the lung tissue of asthma patients, and this upregulation correlated positively with asthma severity; (2) asthma was linked to oxidative stress injury and mitochondrial dysfunction, both of which were alleviated by the absence of ETS2; (3) ETS2 influenced dsRNA expression and its intracellular distribution during asthma; and (4) ETS2 deficiency led to reduced

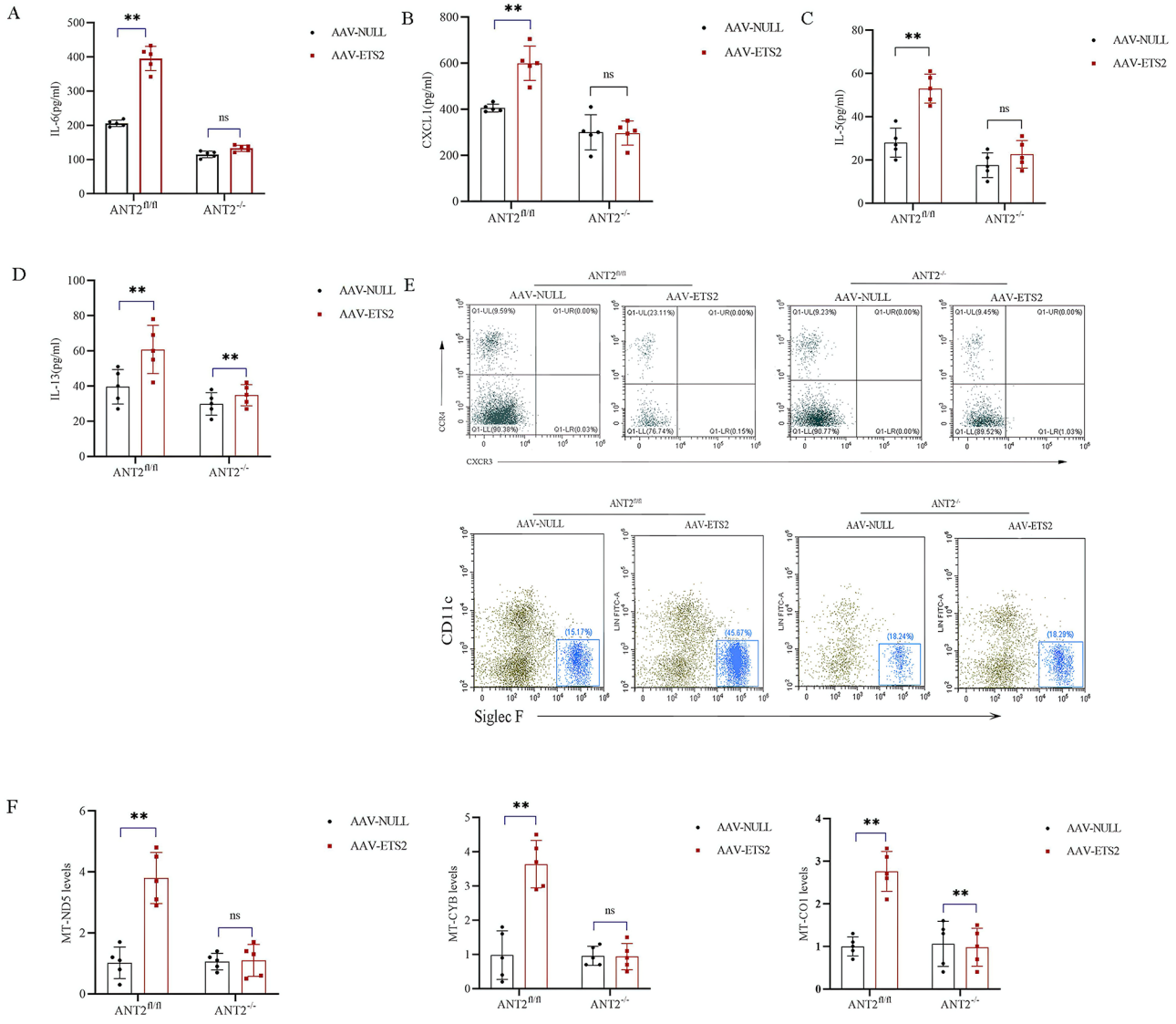

Fig. 7 ETS2 exacerbate asthma development via ANT2. *ANT2*$^{fl/fl}$ mice and *ANT2*$^{fl/fl;Scgb1a1-IRES-cre}$ mice were i.v. injected with AAV9-NULL or AAV9-ETS2, then OVA treated for 30 days. (**A**) IL-6 levels. (**B**) CXCL1 levels. (**C**) IL-5 levels. (**D**) IL-13 levels. (**E**) Flow cytometric plot for the analysis of CD45 + CD4 + CCR4 + CXCR3-Th2 cells and EOS gates as CD45 + CD11c Siglec-F + in the lungs of asthmatic mice. (**F**) mitochondrial dsRNA levels. Data are expressed as mean ± SD. Statistical analysis was performed using two-way ANOVA.ns, not significant. *$P < 0.05$,**$P < 0.01$

ANT2 expression by directly binding to the ANT2 promoter and enhancing its transcription. In conclusion, ETS2 directly modulates ANT2 expression, thereby regulating mitochondrial cross-membrane translocation of dsRNA and exacerbating asthma.

Our findings contrast with earlier work [5] that reported no significant link between ETS2 polymorphisms and asthma susceptibility. This discrepancy may reflect the limitations of genetic association studies in detecting variants with context-dependent or subtle regulatory effects, particularly when focusing on a single disease phenotype (e.g., asthma diagnosis rather than molecular subphenotypes). Here, we demonstrate that ETS2 regulates mitochondrial dsRNA accumulation and downstream cytokine production—a pathway that could contribute to asthma heterogeneity or specific endotypes not stratified in prior genetic analyses. Importantly, our functional approach complements genetic studies by uncovering a previously unappreciated role for ETS2 in mitochondrial-driven inflammation, offering new avenues for targeting ETS2-related pathways in asthma subsets with dsRNA-mediated pathology.

One of the essential roles of ETS2 in inflammatory diseases involves the regulation of immune responses [13]. ETS2 interacts with diverse signaling pathways and transcription factors, thereby influencing the expression of pro-inflammatory cytokines and chemokines [14]. For example, research has shown that ETS2 enhances the

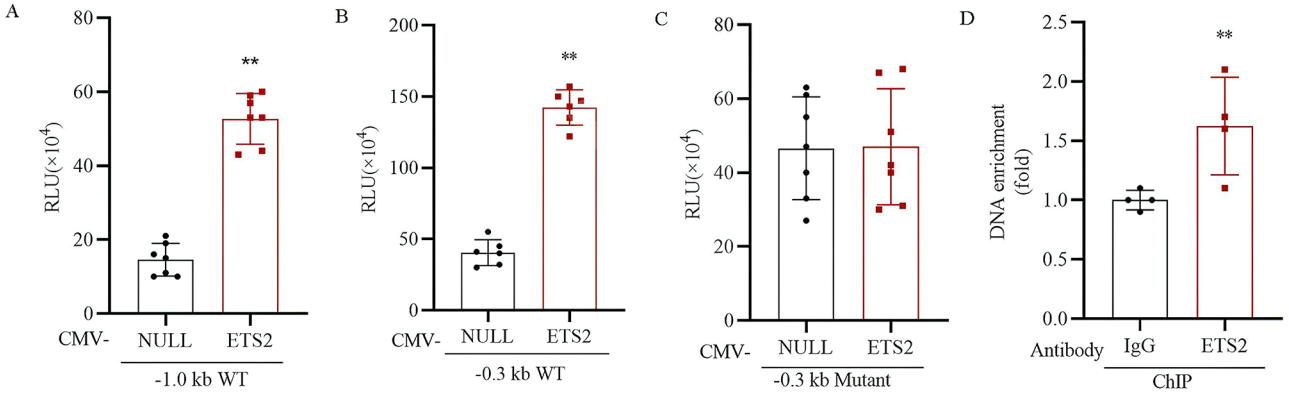

Fig. 8 ANT2 is a direct target of ETS2. (**A**-**C**) Transient transfections were performed by co-transfecting CMV-NULL or CMV-ETS2 with pGL3-ANT2 (-1.0 kb WT) (**A**), pGL3-ANT2(-0.3 kb WT) (**B**) or pGL3-ANT2(-0.3 kb Mutant) (**C**) into BEAS-2B cells ($n=7$). After 24 h, relative luciferase activities (RLU) were determined after normalizing to beta-galactosidase activity. WT, wild-type. (**D**) C57BL/6 mice were i.v. injected with AAV9-NULL or AAV9-ETS2. then OVA treated for 30 days. CHIP assays were performed using lung lysates overexpressing ETS2 and IgG (control) or the ETS2 antibody ($n=4$). The DNA enrichment in the ANT2 promoter was determined by qRT-PCR using primers that amplified a fragment between −227 bp and −154 bp (**D**). Statistical analysis was performed using a 2-tailed, unpaired t-test (**A**-**D**).**$P<0.01$

expression of IL-6, TNF-alpha, and other mediators that are pivotal in the inflammatory response [15]. In conditions such as asthma, characterized by airway inflammation, ETS2's effect on cytokine profiles highlights its significance in promoting the inflammatory processes underlying the disease.

Moreover, the role of ETS2 in facilitating tissue remodeling is particularly significant in chronic inflammatory diseases [16]. In conditions such as asthma and rheumatoid arthritis, persistent inflammation results in structural alterations within tissues, commonly referred to as remodeling. ETS2 regulates the expression of genes involved in extracellular matrix (ECM) production and remodeling, thereby contributing to the progression of these diseases [17]. Targeting ETS2 or its downstream pathways could present a novel strategy for preventing or mitigating tissue remodeling, potentially enhancing patient outcomes.

One of the primary mechanisms by which dsRNA exerts its effects is through pattern recognition receptors (PRRs), particularly Toll-like receptor 3 (TLR3) and the retinoic acid-inducible gene I (RIG-I)-like receptors (RLRs) [18, 19]. Upon detection of dsRNA, these receptors activate downstream signaling cascades, leading to the production of pro-inflammatory cytokines, including interferons (IFNs), IL-6, and TNF-α [20, 21]. In our experiment, cytoplasmic dsRNA levels were found to positively correlate with the expression levels of IL-6, IL-5, and IL-13, and Th2 cytokines were markedly elevated in the lungs.

As ANT2 is located within the inner mitochondrial membrane, it serves a pivotal function in regulating mitochondrial function [22]. Mitochondria serve as the energy-producing organelles of cells, and ANT2 contributes to mitochondrial biosynthesis, energy production, and oxidative phosphorylation by modulating ATP and ADP concentrations [23]. Although ANT2 is primarily recognized for its ATP/ADP transport function, recent research has highlighted its potential involvement in RNA transport. Evidence suggests that ANT2 acts as the mitochondrial inner membrane translocon for RNA translocation, facilitating the cross-membrane movement of RNAs [24, 25]. This function appears to be directly associated with the mitochondrial efflux of dsRNAs, potentially serving as a mechanism underlying various inflammatory diseases.

Our findings also indicate that ANT2 expression is elevated in asthma but is markedly reduced in ETS2-deficient asthma models. This raises the intriguing possibility that the upregulation of ANT2 in asthma may contribute to allergic airway inflammation. Changes in ETS2 levels were shown to impact mitochondrial RNA levels in the cytosol, suggesting that cytosolic dsRNA may directly enhance immune responses in epithelial cells, with ANT2 potentially mediating these processes. Investigating how dsRNA influences the levels of IL-6, IL-5, and IL-13 in epithelial cells will be a critical focus of our future research.

Conclusion

In summary, it was demonstrated that epithelial ETS2 is upregulated in asthma. This upregulation appears to serve a pivotal function in the pathogenesis of asthma. Furthermore, it has been shown that epithelial ETS2 contributes to the progression of asthma by modulating ANT2, and that ETS2 in epithelial cells elevates IL-6, IL-5, and IL-13 levels through ANT2-mediated regulation of mitochondrial dsRNA levels in the cytosol. Therefore, targeting epithelial ETS2 could present a promising strategy for therapeutic interventions in asthma.

Supplementary Information

The online version contains supplementary material available at https://doi.org/10.1186/s12931-025-03233-6.

Supplementary Material 1

Acknowledgements
We would like to thank all the patients who consented to be involved in this study.

Author contributions
H J conceived and designed the study, carried out experiments and analyzed data; Cy F wrote the manuscript and supervised the study. Yn J and R D collecting and tracing patient data. All authors reviewed and edited the final manuscript.

Funding
This work was supported by the National Natural Science Foundation of China (NO.82300121).

Data availability
No datasets were generated or analysed during the current study.

Declarations

Ethics approval and consent to participate
The study was approved by the Ethics Committee of the Tongji Hospital, Tongji University. Participants gave informed consent to participate in the study before taking part.

Consent for publication
Not applicable.

Competing interests
The authors declare no competing interests.

Received: 19 December 2024 / Accepted: 13 April 2025
Published online: 24 April 2025

References

1. Bush A, Kleinert S, Pavord ID. The asthmas in 2015 and beyond: a lancet commission. Lancet. 2015;385:1273–5.
2. Gras D, Chanez P, Vachier I, Petit A, Bourdin A. Bronchial epithelium as a target for innovative treatments in asthma. Pharmacol Ther. 2013;140:290–305.
3. Stankey CT, Bourges C, Haag LM, Turner-Stokes T, Piedade AP, Palmer-Jones C, et al. A disease-associated gene desert directs macrophage inflammation through ETS2. Nature. 2024;630:447–56.
4. Luo Y, Jiang N, May HI, Luo X, Ferdous A, Schiattarella GG, et al. Cooperative binding of ETS2 and NFAT links Erk1/2 and calcineurin signaling in the pathogenesis of cardiac hypertrophy. Circulation. 2021;144:34–51.
5. Baron RM, Palmer LJ, Tantisira K, Gabriel S, Sonna LA, Le L, et al. DNA sequence variants in epithelium-specific ETS-2 and ETS-3 are not associated with asthma. Am J Respir Crit Care Med. 2002;166:927–32.
6. Matkovic Leko I, Schneider RT, Thimraj TA, Schrode N, Beitler D, Liu H-Y, et al. A distal lung organoid model to study interstitial lung disease, viral infection and human lung development. Nat Protoc. 2023;18:2283–312.
7. Qiu X, Hill A, Packer J, Lin D, Ma Y-A, Trapnell C. Single-cell mRNA quantification and differential analysis with census. Nat Methods. 2017;14:309–15.
8. Cao Y, Li Y, Wang X, Liu S, Zhang Y, Liu G, et al. Dopamine inhibits group 2 innate lymphoid cell-driven allergic lung inflammation by dampening mitochondrial activity. Immunity. 2023;56:320–e3359.
9. Hwang B-J, Tsao L-C, Acharya CR, Trotter T, Agarwal P, Wei J, et al. Sensitizing immune unresponsive colorectal cancers to immune checkpoint inhibitors through MAVS overexpression. J Immunother Cancer. 2022;10:e003721.
10. Zecchini V, Paupe V, Herranz-Montoya I, Janssen J, Wortel IMN, Morris JL, et al. Fumarate induces vesicular release of MtDNA to drive innate immunity. Nature. 2023;615:499–506.
11. Ls ADSD, L B et al. J, M T, A R,. Mitochondrial double-stranded RNA triggers antiviral signalling in humans. Nature. 2018 [cited 2024 Oct 10];560. Available from: https://pubmed.ncbi.nlm.nih.gov/30046113/
12. Webb DC, Mahalingam S, Cai Y, Matthaei KI, Donaldson DD, Foster PS. Antigen-specific production of Interleukin (IL)-13 and IL-5 cooperate to mediate IL-4Ralpha-independent airway hyperreactivity. Eur J Immunol. 2003;33:3377–85.
13. Martinez LA. Mutant p53 and ETS2, a Tale of reciprocity. Front Oncol. 2016;6:35.
14. Zhao J, Huang K, Peng H-Z, Feng J-F. Protein C-ets-2 epigenetically suppresses TLRs-induced Interleukin 6 production in macrophages. Biochem Biophys Res Commun. 2020;522:960–4.
15. Ma X, Jiang Z, Li N, Jiang W, Gao P, Yang M, et al. Ets2 suppresses inflammatory cytokines through MAPK/NF-κB signaling and directly binds to the IL-6 promoter in macrophages. Aging. 2019;11:10610–25.
16. van der Pouw Kraan TCTM, Zwiers A, Mulder CJ, Kraal G, Bouma G. Acute experimental colitis and human chronic inflammatory diseases share expression of inflammation-related genes with conserved Ets2 binding sites. Inflamm Bowel Dis. 2009;15:224–35.
17. Trimboli AJ, Cantemir-Stone CZ, Li F, Wallace JA, Merchant A, Creasap N, et al. Pten in stromal fibroblasts suppresses mammary epithelial tumours. Nature. 2009;461:1084–91.
18. Chiappinelli KB, Strissel PL, Desrichard A, Li H, Henke C, Akman B, et al. Inhibiting DNA methylation causes an interferon response in Cancer via DsRNA including endogenous retroviruses. Cell. 2015;162:974–86.
19. Zhang X, Gao R, Zhang C, Teng Y, Chen H, Li Q, et al. Extracellular RNAs-TLR3 signaling contributes to cognitive impairment after chronic neuropathic pain in mice. Signal Transduct Target Ther. 2023;8:292.
20. Oncogenic KRAS. drives immunosuppression of colorectal cancer by impairing DDX60-mediated dsRNA accumulation and viral mimicry - PubMed. [cited 2024 Dec 11]. Available from: https://pubmed.ncbi.nlm.nih.gov/39365875/
21. ADAR. and hnRNPC deficiency synergize in activating endogenous dsRNA-induced type I IFN responses - PubMed. [cited 2024 Dec 11]. Available from: https://pubmed.ncbi.nlm.nih.gov/34297039/
22. Permyakova A, Hamad S, Hinden L, Baraghithy S, Kogot-Levin A, Yosef O, et al. Renal mitochondrial ATP transporter ablation ameliorates Obesity-Induced CKD. J Am Soc Nephrol. 2024;35:281–98.
23. Cho J, Seo J, Lim CH, Yang L, Shiratsuchi T, Lee M-H, et al. Mitochondrial ATP transporter Ant2 depletion impairs erythropoiesis and B lymphopoiesis. Cell Death Differ. 2015;22:1437–50.
24. Wang P, Zhang L, Chen S, Li R, Liu P, Li X, et al. ANT2 functions as a translocon for mitochondrial cross-membrane translocation of RNAs. Cell Res. 2024;34:504–21.
25. Li T, Li Y, Liu T, Hu B, Li J, Liu C, et al. Mitochondrial PAK6 inhibits prostate cancer cell apoptosis via the PAK6-SIRT4-ANT2 complex. Theranostics. 2020;10:2571–86.

Publisher's note